GEOLOGY

Eastern equatorial Pacific cold tongue evolution since the late Miocene linked to extratropical climate

Jingjing Liu[1], Jun Tian[1]*, Zhonghui Liu[2]*, Timothy D. Herbert[3], Alexey V. Fedorov[4], Mitch Lyle[5]

The timing and mechanisms of the eastern equatorial Pacific (EEP) cold tongue development, a salient feature of the tropical ocean, are intensely debated on geological time scales. Here, we reconstruct cold tongue evolution over the past 8 million years by computing changes in temperature gradient between the cold tongue and eastern Pacific warm pool. Results indicate that the cold tongue remained very weak between 8 and 4.3 million years ago, implying much weaker zonal temperature gradients prevailing during the late Miocene–Pliocene, but then underwent gradual intensification with apparently increasing sensitivity of the cold tongue to extratropical temperature changes. Our results reveal that the EEP cold tongue intensification was mainly controlled by extratropical climate.

INTRODUCTION

The modern tropical Pacific is characterized by a zonally asymmetric pattern of sea surface temperature (SST) distribution along the equator with a warm pool in the west and a cold tongue (CT) in the east. By modulating atmospheric heat and moisture transport from low to high latitudes, the eastern equatorial Pacific (EEP) CT greatly affects modern climate variability on time scales from seasonal to interannual to decadal (*1*, *2*). Cool EEP subsurface water, originating from subduction of surface water in extratropical regions (*3*–*5*), upwells to the surface and thus regulates heat distribution within the ocean. The CT region is characterized by a strong atmospheric subsidence that exerts powerful controls on global circulation patterns and the position of the intertropical convergence zone (ITCZ) (*6*). The CT region is also one of the largest natural oceanic sources of atmospheric CO_2 contributing to global carbon cycle (*7*).

However, the timing and mechanisms of the CT development into its modern state are controversial. Records of EEP thermocline depth/temperature that should, in principle, affect CT surface conditions indicate gradual thermocline shoaling between the early Pliocene and the present, with a particular strong subsurface cooling between 4.8 and 4.0 million years (Ma) ago (*8*, *9*). The CT development is also associated with the contraction of the Pacific warm pool and the strengthening of the meridional SST gradient (*10*). A simple hypothesis combining ocean dynamics and ocean-atmosphere interaction suggests that the zonal SST gradient between the eastern and western Pacific and meridional SST gradient between the tropics and extra-tropics should be tightly linked (*11*, *12*). Most of the available zonal and meridional gradient records generally support reduced SST gradients and, by inference, a weak CT during the Pliocene warm period (5 to 3 Ma ago) (*10*–*15*). This state is often referred to as "permanent El Niño–like" conditions (*13*, *14*, *16*), although contrasting views also exist (*17*, *18*). However, the exact timing of when the CT first emerged or reached modern-like strength is difficult to assess because of uncertainties in proxy temperature data and difficulties in calculating temperature gradients using heterogeneous proxy datasets.

Two major hypotheses have been proposed to explain the CT strengthening relative to the rest of the tropical Pacific since the early Pliocene—a gradual surface cooling in the extratropical Pacific (*3*, *11*, *12*) and the closure of Central American seaway (CAS) (*8*). The former hypothesis reliably produces CT strengthening if an extratropical cooling is imposed in climate simulations. In contrast, model simulations (*13*, *19*) indicate that an open CAS has a relatively small effect on equatorial SSTs so that CAS changes can influence CT only indirectly, for example, by modifying the tropical thermocline (*8*, *20*). Reliable reconstructions of the CT thermal history are necessary to reconcile these ideas.

Here, to describe the CT development over the past 8 Ma, we use the SST gradient between the eastern Pacific warm pool (EPWP) and the CT core area (Materials and Methods; fig. S1) based on an internally consistent proxy dataset (alkenone estimates of SST). The SST gradient between the EPWP and CT increases during La Niña events but decreases during El Niño, especially during extreme El Niño events (*1*), closely matching the expansion and contraction of the EEP CT. By focusing on this region, we avoid deficiencies of multiproxy approaches that infer CT evolution from SST gradients between the EEP and the western Pacific warm pool, with estimates for the Pliocene ranging from nearly 1° (*11*, *13*, *14*, *21*) to ~3°C (*17*, *18*) and thus implying quite different CT states. In addition, computing the SST gradient between the relatively close EPWP and CT core effectively removes cooling or warming variability unrelated to the development of the CT that may be encapsulated in SST gradients estimated between more distant regions (because of different magnitudes of SST changes) or in individual EEP SST records. We have generated an 8-Ma alkenone-SST record at Integrated Ocean Drilling Program (IODP) site U1337 (3°50.009′N, 123°12.352′W; 4463-m water depth; Fig. 1) and used the alkenone-based SST record (*22*, *23*) from site 846, with the highest data resolution, to represent SST evolution in the CT core area. Other alkenone records from the eastern Pacific (*17*, *24*–*26*) are also examined to ensure the overall data consistency. SSTs were adjusted for paleolocation migration following the procedures of Herbert *et al.* (*23*) (table S1). Site chronology, alkenone analysis, proxy calibration, SST correction for site migration, and potential limitations in our approach are addressed in Materials and Methods and the Supplementary Materials.

[1]State Key Laboratory of Marine Geology, Tongji University, Shanghai 200092, China. [2]Department of Earth Sciences, The University of Hong Kong, Hong Kong, China. [3]Department of Earth, Environmental and Planetary Sciences, Brown University, Providence, RI 02912, USA. [4]Department of Geology and Geophysics, Yale University, New Haven, CT 06520, USA. [5]College of Earth, Ocean, and Atmospheric Sciences, Oregon State University, Corvallis, OR 97331, USA.
*Corresponding author. Email: tianjun@tongji.edu.cn (J.T.); zhliu@hku.hk (Z.L.)

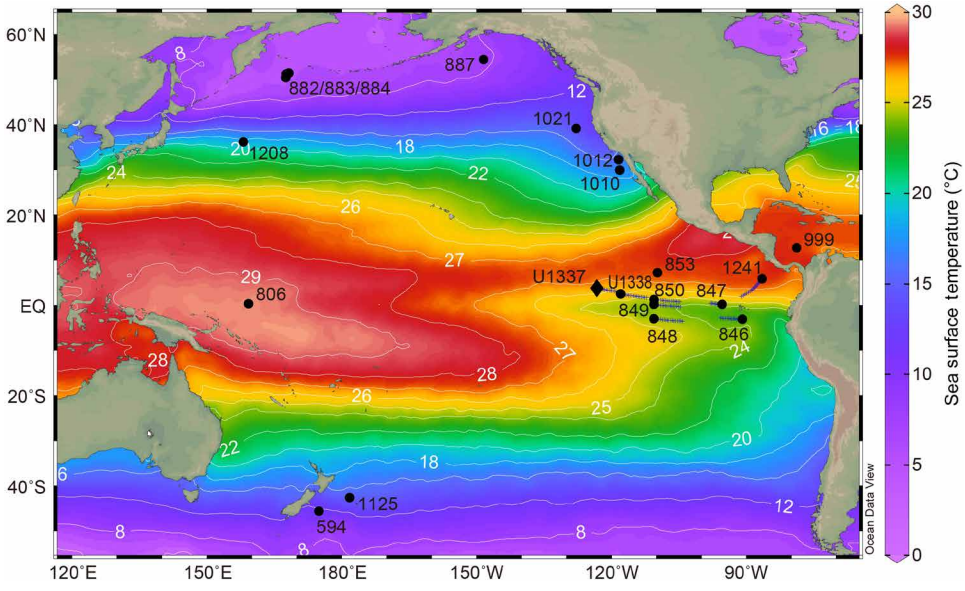

Fig. 1. Location map of the studied sites, superimposed on modern SST field. All the sites are IODP/ODP/Deep Sea Drilling Project (DSDP) sediment cores. Site U1337 is indicated with a diamond, and sites used or cited are indicated with circles. Annual mean SST (colors and contours) was retrieved from World Ocean Atlas (WOA) 2013. The cross lines indicate backtracks of the tectonic movement of the studied eastern Pacific sites over the past 8 Ma (in 0.5-Ma steps).

RESULTS

Our new SST record from site U1337 (table S2) shows a marked similarity in structure to those from other sites in the eastern Pacific (Fig. 2; original SST records uncorrected for site migration are shown in fig. S2). SST values at this site stayed around 28.5° to 29°C between 8 and 7 Ma ago, entered the late Miocene global cooling (LMC) period (7 to 5.4 Ma ago) (*23*) with gradual cooling of ~1° to 1.5°C, rebounded at ~5.5 Ma ago, and stayed above 28°C until ~4.3 Ma ago. After 4.3 Ma ago, the long-term cooling trend began, with increased short-term variability into the Pleistocene period culminating in cooling of ~2.5°C. The same overall structure can be recognized in other EEP SST records (sites 846, 847, 850, and U1338), especially the high-resolution record from site 846 (Fig. 2), which shows ~4° to 6°C cooling toward the present. As all records except that from site 846 are undersampled with respect to orbital variability, we expect some degree of aliasing in assessing the timing of long-term changes. However, at these sites (except for site 850), their Pleistocene mean SSTs show a pattern of decreasing values toward the CT core area, consistent with their modern SST distribution (Fig. 1), and subtle SST differences between the EPWP and EEP sites persist even during the warm Pliocene period (Fig. 2), suggesting minimal interlaboratory analytical bias and the fidelity of the alkenone-SST proxy.

To remove the global cooling effect from SST records, we compute the SST gradient between EEP site 846 and EPWP site U1337, $\Delta SST_{1337-846}$ (Materials and Methods; Fig. 2C), which effectively captures the CT development. A turning point in $\Delta SST_{1337-846}$ can be identified at 4.32 ± 0.16 Ma ago, with individual SST records at sites 846 and U1337 identified at 4.04 ± 0.04 Ma ago and 4.29 ± 0.14 Ma ago, respectively (fig. S3). Before this turning point at around 4.3 Ma ago, $\Delta SST_{1337-846}$ values generally stayed around 1°C, ranging from 0.5°C during warm intervals to 2°C during cool intervals (Fig. 2C), with a very weak long-term increasing trend (0.15°C/Ma). After ~4.3 Ma ago, $\Delta SST_{1337-846}$ values gradually increased from ~3° to 5°C toward the present (Fig. 2C), close to its modern value (2.6°C; fig. S1 and table S3), with a strong trend (0.67°C/Ma) evident. Alternative alkenone calibration equations do not alter the structure in $\Delta SST_{1337-846}$ and individual SST records, although their absolute values are affected (Materials and Methods; fig. S4).

To place $\Delta SST_{1337-846}$ values into the context of modern observations, we note that the SST gradient between the two sites is 1.5°C for boreal winter [December to February (DJF)] and 2.6°C for annual mean over the 1980–2010 period; during the strongest on record El Niño event of 1997/1998, this gradient decreased to 0.5°C for winter months and to 1.2°C for annual mean (August 1997 to July 1998) (fig. S1 and table S3). Our $\Delta SST_{1337-846}$ record, interpreted as the difference in annual mean SSTs (Materials and Methods), indicates that an EEP CT similar to, or even weaker than, that during the 1997/1998 winter may have characterized warm intervals before 4.3 Ma ago. Hence, the mean SST gradient before 4.3 Ma ago (below 1°C) indicates that the CT was weaker than modern winter (DJF, 1.5°C) and annual mean (2.6°C) conditions, and even weaker than 1997/1998 annual values (1.2°C) (fig. S1 and table S3), approaching the 1997/1998 winter strength between ~6.2 and 8 Ma ago. If the 1997/1998 El Niño state were used as a limited analog for Pliocene warm ocean conditions (Fig. 2), then one would estimate the Pliocene zonal SST gradient between western Pacific (site 806) and EEP (site 846) as 0.4°C (winter months) or 1.4°C (annual mean), much smaller than the modern mean annual or winter gradient, ~5°C (table S3). Thus, the CT was very weak before 4.3 Ma ago; it then gradually intensified and reached modern values around ~0.8 Ma ago (Fig. 2C and fig. S3).

DISCUSSION

Although the alkenone ratio is considered a reliable temperature proxy, it should be used with caution when the unsaturation ratio approaches unity. Absolute SST values cannot be accurately derived for Pliocene warm pool waters, especially for the western Pacific (*17*, *23*). To a lesser degree, the near-saturation issue also applies to

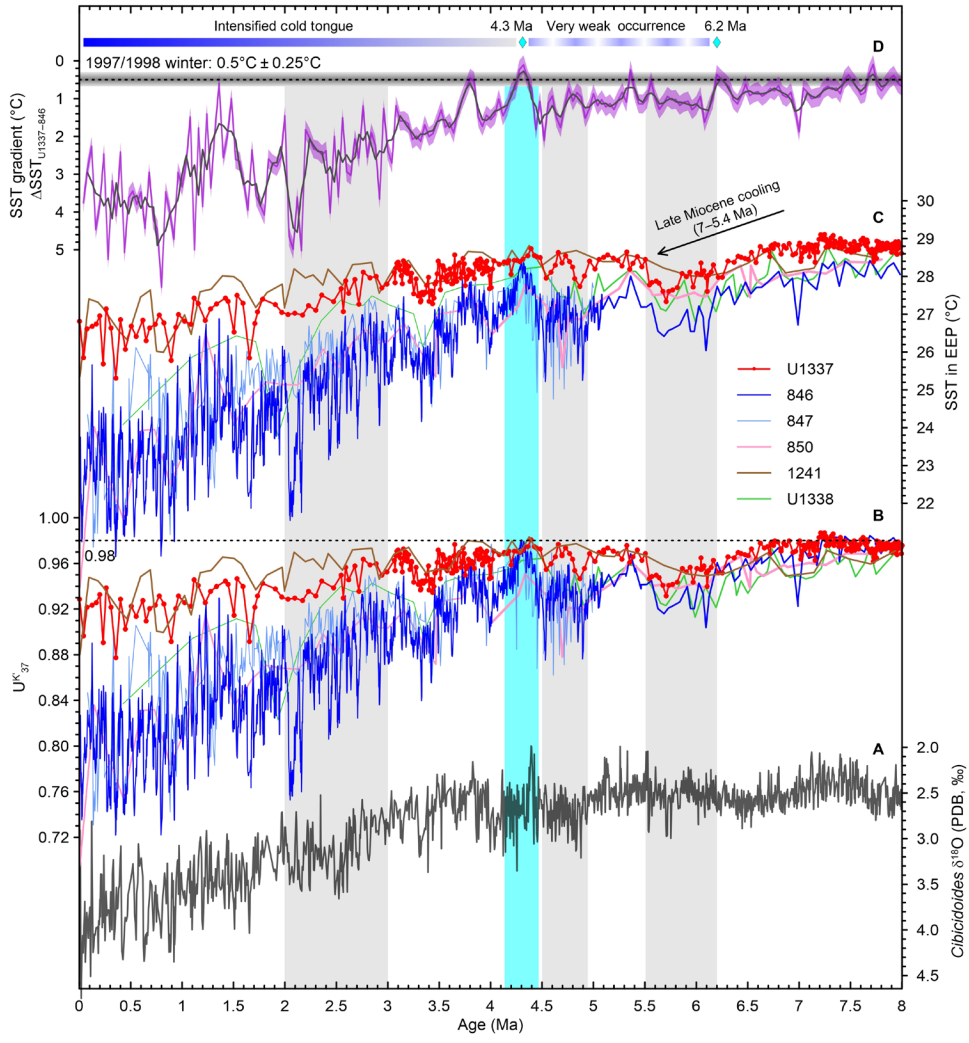

Fig. 2. SST records from the eastern Pacific and the new construction of EEP CT development. (**A**) Benthic foraminiferal $\delta^{18}O$ of site U1337 (*47*) for reference. PDB, Pee Dee Belemnite. (**B**) Original $U^{K'}_{37}$ time series at IODP sites U1337 and U1338 and ODP sites 846, 847, 850, and 1241, with the dashed line indicating high $U^{K'}_{37}$ values (~0.98) between ~4 and 8 Ma ago. (**C**) Calculated SST changes at those sites. (**D**) $\Delta SST_{U1337–846}$, the SST gradient between sites U1337 and 846, with the black line denoting three-point running means and the pink shaded area indicating estimate uncertainty (±0.25°C). The dashed line highlights the $\Delta SST_{U1337–846}$ value (0.5°C) for winter months in the 1997/1998 El Niño event. SST and $\Delta SST_{U1337–846}$ values in (C) and (D) were corrected for site migration over the past 8 Ma. SST data are from (*17*, *22*–*26*) and this study.

Pliocene SST estimates in the eastern Pacific, including our study site U1337. However, the alkenone proxy is still capable of indicating relative temperature changes during the warm Pliocene period, as demonstrated by the similar subtle features shared at all the EEP sites (Fig. 2). Furthermore, our approach in this study relies on the SST difference between the EPWP and EEP, not the absolute SST values. Because higher ratios (0.99 to 1.00) occurred before ~10 Ma ago in the two longer records from sites 846 and U1338 (*23*, *26*), the almost identical ratios (~0.98) at warm intervals between ~3 and 8 Ma ago at the EEP sites (Fig. 2 and fig. S2) would certainly indicate minimal temperature contrast among those paleolocations, not a result of the near-saturation issue (Materials and Methods; figs. S4 and S5). Therefore, we assess that the very weak CT occurrence inferred here is largely unaffected by the alkenone proxy uncertainty.

Quantification of basin-wide zonal SST gradient in the Pliocene (3 to 5 Ma ago) tropical Pacific remains to be challenging due to various proxy uncertainties (fig. S6). Notably, uncertainty in past seawater Mg/Ca ratio affects Mg/Ca-SST reconstruction (*18*, *27*, *28*). The alkenone proxy is subject to the near-saturation issue (*17*), whereas the TEX_{86}-SST proxy might contain subsurface signal particularly in tropical waters, as demonstrated in previous studies of the Last Glacial Maximum period (*29*, *30*). On the basis of existing data, Mg/Ca-SST estimates (*14*) from sites 806 and 847 (Fig. 1), whether corrected for past seawater Mg/Ca changes or not (*18*, *28*, *31*), suggest a weak Pliocene gradient (~1° to 1.5°C). Alkenone-SST estimates from sites 806 (*17*), 846 (*22*, *23*), and U1337 in this study, with the conventional alkenone calibration (*32*), also tend to suggest a weak gradient, ~2°C ($\Delta SST_{806–846}$) or ~1°C ($\Delta SST_{806–1337}$), which is perhaps affected by the alkenone near-saturation issue and the low-resolution data at site 806. On the other hand, the TEX_{86}-SST estimates from sites 806 and 850 (*17*), with the conventional TEX_{86} calibration (*33*), give a rather large SST gradient (~3.2°C). With the recently proposed Bayesian calibrations for the alkenone and TEX_{86} proxies (*34*, *35*), the alkenone-based gradient further increases to ~3.5°C ($\Delta SST_{806–846}$)

or ~1.5°C ($\Delta SST_{806-1337}$), while the TEX_{86}-based gradient remains the same (~3.2°C) (fig. S6). All the estimates are smaller than the modern mean (fig. S1 and table S3) and thus suggest reduced Pliocene zonal gradient, but the large range from nearly 1° to ~3.5°C implies quite different CT status during the warm Pliocene period. The very weak CT occurrence inferred here supports a relatively weak basin-wide zonal SST gradient and thus provides further constraint to the ongoing debate on this outstanding issue.

To assess linkages between the CT development, extratropical cooling, and CAS closure, we now examine our new CT reconstruction (Fig. 3D) together with zonal (Fig. 3C) and meridional SST gradients (Fig. 3B), and EEP thermocline depth/temperature records (Fig. 3E). The structure of $\Delta SST_{1337-846}$ largely mimics that of individual SST records and zonal and meridional SST gradients (Fig. 3), at least over the past 5 Ma, but with further constraints on detailed

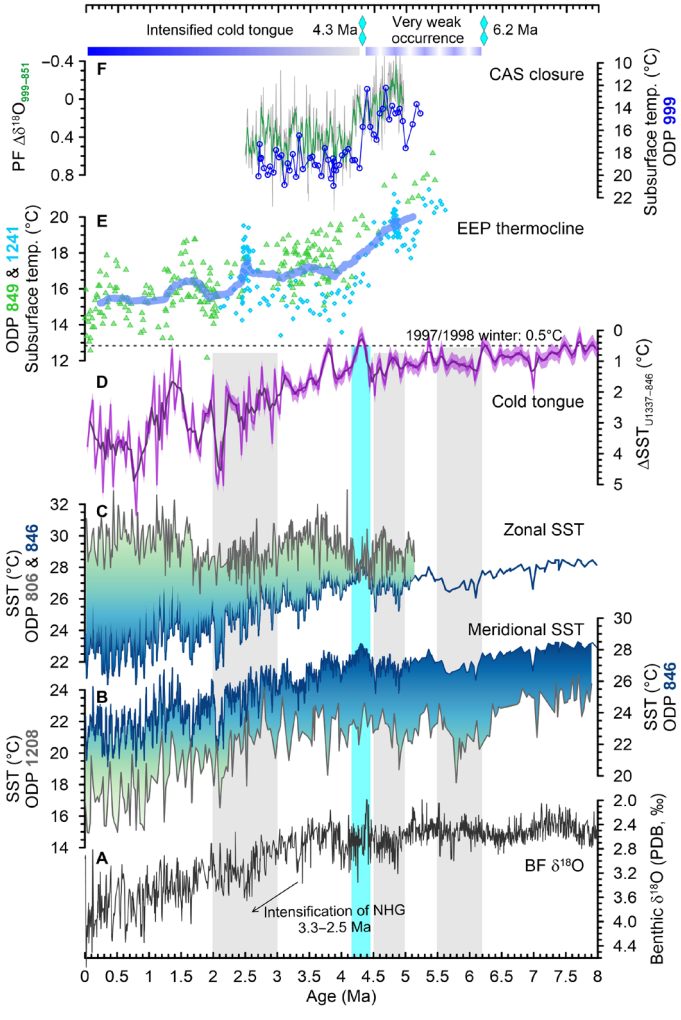

Fig. 3. EEP CT development compared with other representative surface and subsurface records. (**A**) Benthic foraminiferal $\delta^{18}O$ of site U1337 (*47*). (**B**) Meridional SST gradient between sites 846 and 1208. (**C**) Zonal SST gradient between sites 806 and 846. (**D**) $\Delta SST_{U1337-846}$. (**E**) Mg/Ca subsurface temperature records at ODP sites 849 and 1241. (**F**) $\Delta\delta^{18}O_{999-851}$, the $\delta^{18}O$ difference between ODP sites 851 and 999, with the green line denoting three-point running mean, and subsurface temperature at site 999. NHG, the Northern Hemisphere Glaciation; BF, benthic foraminiferal; PF, planktonic foraminiferal. SST data are from (*14*, *22*, *23*, *52*), and $\delta^{18}O$ [in (F)] and subsurface data are from (*8*, *9*, *37*). A more completed display can be found in figs. S2, S6, and S7.

CT development during the Pliocene that enables us to evaluate the two main proposed mechanisms (*3*, *8*, *12*). In line with previous analyses (*11*, *13*, *23*), most of the records convincingly show that the stronger CT development since ~4.3 Ma ago was accompanied by a gradual global cooling and increased zonal and meridional SST gradients (figs. S2, S6, and S7). Around ~4.3 Ma ago, the very weak CT state co-occurs with warmer SSTs and reduced zonal and meridional SST gradients (Fig. 3). Before 4.3 Ma ago, perhaps because of relatively weak signals, low-resolution data, and chronological uncertainty, the identified maximal meridional SST gradient in these records does not always occur during the LMC period (figs. S2 and S7). However, in light of the recently reported globally synchronous LMC (*23*) at 7 to 5.4 Ma ago and theoretical/modeling inference that tropical Pacific zonal SST gradient should be tightly connected to meridional SST gradients (*11*), these surface components should have shared some similarities in structure even before 4.3 Ma ago.

Unexpectedly, the evolution of EEP thermocline shoaling/cooling displays a rather different structure. A slow cooling trend (Fig. 3E) after ~4 Ma ago is in concert with other surface processes (Fig. 3, B to D), but a strong shoaling trend occurred from 5.5 to 4.0 Ma ago, corroborated with the $\delta^{18}O$ records of subsurface dwelling planktonic foraminifera in the western Pacific (*14*) and EEP (*9*). This feature is in contrast with the weak CT state inferred here and other surface conditions (warm SSTs and reduced SST gradients) centered on ~4.3 Ma ago (Fig. 3 and fig. S7). A deeper EEP thermocline before 4.3 Ma ago, indicated by substantially warmer thermocline temperatures (Fig. 3E) (*8*, *9*, *36*), suggests that the dissociation of surface CT to thermocline depth may have occurred. Currently, most of the subsurface records terminate at 5 or 5.5 Ma ago, leaving the thermocline behavior during the cool LMC (7 to 5.4 Ma ago) undocumented, from which the dissociation status before ~4.3 Ma ago could be further examined.

The two current hypotheses, a sufficiently deep open CAS (*8*) and extratropical warmth (*3*, *12*), could both account for the deep EEP thermocline. With the thermocline tunneling mechanism (*3*, *11*, *12*), the overall extratropical warmth before 4.3 Ma ago (fig. S2) can explain the deep EEP thermocline. However, our new reconstruction shows stronger CT development from 3 to 2 Ma ago than the LMC, while extratropical SST changes were similar for the two periods (Fig. 3 and fig. S2) (*23*), which requires further examination. Previous records (*8*, *9*, *37*) show an increased planktonic $\delta^{18}O$ gradient between the EEP and Caribbean Sea, reduced thermocline temperatures in the EEP, and increased subsurface temperatures in the Caribbean Sea around ~4.2 Ma ago, indicating that the CAS closure reached its final stage or a critical threshold (Fig. 3F and fig. S7E). Therefore, the overall extratropical warmth, perhaps with additional contribution from a partially open CAS before 4.3 Ma ago, may have resulted in the deep EEP thermocline, causing some dissociation with surface CT development (Fig. 3).

We conclude that the EEP CT exhibits two stages of development with a turning point around ~4.3 Ma ago (fig. S3). Before ~4.3 Ma ago, the very weak CT occurrence and its dissociation with the deep EEP thermocline suggest a reduced SST sensitivity to the thermocline tunneling mechanism (*3*, *11*, *12*). The weak CT development during the LMC (7 to 5.4 Ma ago) as compared to 3 to 2 Ma ago, when considering the extratropical cooling during the two periods (*23*), may also suggest a relatively small contribution from the tunneling mechanism. Yet, the CT development still shows some resemblance to extratropical SSTs and meridional SST gradients (Fig. 3 and fig. S7), indicating that some surface processes may have contributed to this linkage.

Before ~4.5 Ma ago, high levels of biogenic production during the late Miocene biogenic bloom (LMBB) (*38*–*40*) in the EEP suggest substantial flow of nutrients into surface waters. Strong upwelling (*41*) along with the very weak CT development before ~4.3 Ma ago could have occurred only if the upwelled waters were relatively warm. There is also a dissociation between biogenic sediment burial and development of the CT. The LMBB in the EEP could be interpreted as part of the global carbon cycle perturbations (*23*, *40*), resulting from increased terrestrial nutrient input (*40*) or nutrient redistribution within ocean basins from oceanic reorganization (*39*). After the LMBB, high biological productivity shifted east toward the easternmost Pacific (*38*). Site 846 provides another example of EEP surface production largely independent of SST change or CT development. Higher biological production occurred between 3 and 1.5 Ma ago than <1.5 Ma ago at site 846, while SST continued to cool and CT further developed through the Pleistocene (*22*).

Around ~4.3 Ma ago, when the CAS closure reached a critical threshold and the EEP thermocline shoaled substantially (Fig. 3), the very weak CT development can only be attributed to warm extratropical SSTs (*23*). Afterward, the tight linkage among the extratropical SSTs, thermocline temperature, and CT development (Fig. 3), perhaps even on orbital time scales [e.g., (*42*)], would imply the dominant control of extratropical cooling on the CT intensification through the thermocline tunneling mechanism. The accelerated extratropical cooling and CT development since ~4.3 Ma ago are significantly correlated with R^2 = ~0.5 [for both mid- and high-altitude SST stack (*23*)]. Steph *et al.* (*8*) suggest that the CAS closure may have triggered northern hemisphere warming but southern hemisphere cooling, northward shift of the ITCZ, southeasterly trade wind intensification, shoaling of the EEP thermocline, and the consequent CT development. However, the synchronous hemispheric SST changes inferred from recently available global SST datasets (*23*) and the surface CT development inferred here (Fig. 3) do not support the proposed chain processes (*8*). The close correspondence of CT development to extratropical SSTs and zonal and meridional SST gradients since ~4.3 Ma ago thus favors the hypothesis of surface cooling in extratropical regions and thermocline tunneling for the CT development (*3*, *11*, *12*).

In summary, our new reconstruction of the EEP CT development thus clarifies current controversies on the tropical Pacific zonal SST gradient during the warm Pliocene epoch (*10*, *11*, *13*, *14*, *17*, *18*, *21*). The very weak CT development before ~4.3 Ma ago, or even before 3 Ma ago, implies much reduced zonal SST gradient at the time. During much of the Pliocene period, tropical Pacific zonal SST gradient may have been similar to the weak gradient characteristic of the strong 1997/1998 El Niño event. With the close linkages established after ~4.3 Ma ago when the CAS closure reached a critical threshold (*8*, *37*), we conclude that the EEP CT intensification was controlled by extratropical surface cooling through the thermocline tunneling mechanism (*3*, *11*, *12*) and may also have contributed to the accelerated global cooling because of the tightened connections between high and low latitudes (*2*).

MATERIALS AND METHODS

Oceanic setting

The EPWP (Fig. 1 and fig. S1) plays an important role in the CT evolution, including its associated regional and global teleconnections, based on modern observations and model simulations (*43*). In the EPWP, large latitudinal movement of site 1241 over the past 8 Ma renders the very low-resolution SST record from this site (*25*) unsuitable for this study. Site U1337 is currently located near the 27°C isotherm of the EPWP, and remained out of the equatorial upwelling zone during the investigated period (Fig. 1), and thus used in this study.

We recognized that site U1337 was also influenced by the CT in modern settings and the gradient between sites 846 and U1337 ($\Delta SST_{1337-846}$) was relatively small as compared to the defined gradient index between the EEP and EPWP (*1*). Furthermore, because of their longitudinal distance, $\Delta SST_{1337-846}$ would also partly reflect the tropical Pacific basin-wide zonal SST gradient. Modern annual mean $\Delta SST_{1337-846}$ is 2.6°C (fig. S1) versus 3.8°C for $\Delta SST_{1241-846}$ and 5.2°C for $\Delta SST_{806-846}$ (Fig. 1 and table S3). Therefore, as most intense gradients developed to the east of site U1337, where SST records from multiple sites are available in this study (*17*, *24*, *26*), our approach would still effectively capture the CT variation, especially its early development.

Modern SST values were retrieved from World Ocean Atlas (WOA) 2013 (*44*) and the simple ocean data assimilation (SODA) dataset (*45*) and plotted with Ocean Data View (*46*). We compared $\Delta SST_{1337-846}$ values during the warm Pliocene epoch with modern climatological means and those during the strong 1997/1998 El Niño event using both boreal winter (DJF) and annual mean values and acknowledging that seasonality during the warm Pliocene epoch might differ substantially from the modern EEP one.

Alkenone analysis

We analyzed 382 samples from IODP site U1337, yielding an average resolution of 20 to 40 ka over the past 8 Ma, based on $\delta^{18}O$ stratigraphy (*47*). Sediment samples (~5 to 20 g of dry weight) were grounded, freeze-dried, and extracted with organic solvents (dichloromethane/methanol = 9:1, v/v). After being saponified with 6% KOH in methanol solution, lipids were separated into three fractions with silica gel column chromatography. The alkenone fraction was analyzed on Agilent 7890 GC equipped with a flame ionization detector and an HP DB-1 capillary column. *n*-C_{36} alkane was used as external standard for alkenone quantifications. Analytical precision (1σ) for our laboratory standards is 0.005 unit (equivalent to 0.1° to 0.2°C) for the alkenone unsaturation index, $U^{K'}_{37} = [C_{37:2}]/([C_{37:2}] + [C_{37:3}])$, where $[C_{37:2}]$ and $[C_{37:3}]$ are contents of di- and tri-unsaturated C_{37} alkenones, respectively, and 5% for alkenone content. The global core-top temperature calibration (*32*) ($U^{K'}_{37} = 0.033T + 0.044$) was used to convert the index into annual mean SST values. Other available alkenone records from the region, if different calibration equations were used previously, were also recalibrated using the same equation (*32*). As seasonal variability in primary production was very weak in the open-ocean EEP (*48*), we expected minimal seasonal bias in the alkenone proxy, representing annual mean SSTs in the region.

Analysis of replicated samples indicated that analytical precision is equivalent to ~0.2°C. We noted that $U^{K'}_{37}$ values from U1337 Pliocene/late Miocene samples, similar to other alkenone records from the eastern Pacific (*17*, *22*–*26*), were at high end (0.93 to 0.99) but had not yet reached unity over the past 8 Ma. Because of characteristically small $C_{37:3}$ peaks, we expected uncertainty in $C_{37:3}$ quantification in these samples. However, even with a 20% uncertainty (a substantial overestimate) in $C_{37:3}$ quantification, $U^{K'}_{37}$ values in such samples (for example, $U^{K'}_{37} = 0.95$) would change only by 0.01 unit, equivalent to 0.3°C. We thus assessed that, although $U^{K'}_{37}$ values

approaching unity may not accurately reflect their absolute temperatures, their relative SST changes were still robust. An alternative BAYSPLINE alkenone temperature calibration (*34*) yielded warmer SSTs by up to ~2°C toward the $U^{K'}_{37}$ unity (with a notably greater 1σ error of ~4°C), but the structure of SST changes remained (fig. S4).

To investigate the possibility of potential capping of the signal between 3 and 8 Ma ago due to the upper limit of the $U^{K'}_{37}$ thermometer, we isolated higher-frequency variations in the signal, predominantly associated with glacial cycles and noise, by subtracting a five-point running mean and a five-point weighted mean from the record. Analyzing the resulting high-frequency anomalies showed that there was no discernible difference between temperature increases and decreases, i.e., the distribution of anomalies was nearly Gaussian with close to zero skewness (fig. S5). A negative skewness would have implied a lower probability of temperature increases or "capping."

SST gradient calculation

$\Delta SST_{1337-846}$ was calculated by subtracting the evenly interpolated SST record of ODP site 846 to 40-ka spacing from that of IODP site U1337. Interlaboratory biases seemed to be minimal as Pleistocene mean values from EEP sites generated by various laboratories were consistent with their modern SST distribution patterns (Fig. 1). SST values at sites U1337 and 1241, indistinguishable before 4.3 Ma ago, consistently showed more divergence from the EEP sites (846, 847, 850, and U1338) during relatively cool intervals, indicated by both benthic $\delta^{18}O$ (Fig. 2A) and SST (Fig. 2C) records, notably during 5.5 to 6.2 Ma ago (LMC) and 4.5 to 4.9 Ma ago, and remained close (within ~0.5°C) during warm intervals, indicating the persistency of subtle SST differences between the EPWP and EEP.

In this study, we applied 0.3°C as uncertainty for calculated SST values, larger than the typical analytical uncertainty of ~0.2°C achieved in our laboratory, to account for potential uncertainties in those high SST estimates. The estimated uncertainty in $\Delta SST_{1337-846}$ is thus ~0.5°C, including potentially slight misalignment of the two SST records due to chronological uncertainty and estimate bias due to data resolution changes. We noted that, at warm intervals before 4.3 Ma ago, alkenone $U^{K'}_{37}$ values were almost identical (within uncertainty) at the two sites. Thus, the calculated $\Delta SST_{1337-846}$ value at warm intervals was irrespective of calibration equations used and the SST difference between the two sites largely resulted from the correction for site migration (Supplementary Materials). At cool intervals before ~4.3 Ma ago, the BAYSPLINE calibration (*34*) yielded greater $\Delta SST_{1337-846}$ values by up to ~1°C than the global core-top calibration (fig. S4) (*32*). However, it also resulted in further deviation of the calculated topmost $\Delta SST_{1337-846}$ value from modern observation (~4.5°C versus 2.6°C). For these reasons, we here adopted the global core-top calibration (*32*) to make comparisons with modern observations.

SUPPLEMENTARY MATERIALS

Supplementary material for this article is available at http://advances.sciencemag.org/cgi/content/full/5/4/eaau6060/DC1

Supplementary Text

Fig. S1. Modern SST distribution in the EEP.

Fig. S2. Existing Pacific SST records covering the Pliocene-Pleistocene period, in comparison with the new CT reconstruction ($\Delta SST_{1337-846}$).

Fig. S3. Turning points in $\Delta SST_{1337-846}$ and U1337 and 846 SST records determined by RAMPFIT.

Fig. S4. Comparisons of SST and $\Delta SST_{1337-846}$ reconstructions with alternative calibration equations.

Fig. S5. The frequency distribution of SST anomalies between 3 and 8 Ma ago from site U1337.

Fig. S6. Tropical SST contrast between the western and eastern Pacific from various proxies.

Fig. S7. Various versions of reconstructed meridional SST gradients and EEP thermocline.

Table S1. Applied SST correction for paleolocation migration at sites 846, 847, 850, 1241, U1337, and U1338.

Table S2. SST records from sites U1337, 846, U1338, 850, 847, and 1241, with corrections applied, and SST gradient between sites U1337 and 846 based on two calibrations.

Table S3. Observed SST gradients among sites 806, 1241, U1337, and 846 in modern period.

References (*49*–*51*)

REFERENCES AND NOTES

1. W. Cai, S. Borlace, M. Lengaigne, P. van Rensch, M. Collins, G. Vecchi, A. Timmermann, A. Santoso, M. J. McPhaden, L. Wu, M. H. England, G. Wang, E. Guilyardi, F.-F. Jin, Increasing frequency of extreme El Niño events due to greenhouse warming. *Nat. Clim. Chang.* **4**, 111–116 (2014).
2. S. Hu, A. V. Fedorov, The extreme El Niño of 2015–2016 and the end of global warming hiatus. *Geophys. Res. Lett.* **44**, 3816–3824 (2017).
3. S. G. Philander, A. V. Fedorov, Role of tropics in changing the response to Milankovich forcing some three million years ago. *Paleoceanography* **18**, 1045 (2003).
4. S. Harper, Thermocline ventilation and pathways of tropical–subtropical water mass exchange. *Tellus A* **52**, 330–345 (2000).
5. J. L. Sarmiento, N. Gruber, M. A. Brzezinski, J. P. Dunne, High-latitude controls of thermocline nutrients and low latitude biological productivity. *Nature* **427**, 56–60 (2004).
6. A. Koutavas, J. Lynch-Stieglitz, in *The Hadley Circulation: Present, Past and Future* (Springer, 2004), pp. 347–369.
7. T. Takahashi, S. C. Sutherland, R. Wanninkhof, C. Sweeney, R. A. Feely, D. W. Chipman, B. Hales, G. Friederich, F. Chavez, C. Sabine, A. Watson, D. C. E. Bakker, U. Schuster, N. Metzl, H. Yoshikawa-Inoue, M. Ishii, T. Midorikawa, Y. Nojiri, A. Körtzinger, T. Steinhoff, M. Hoppema, J. Olafsson, T. S. Arnarson, B. Tilbrook, T. Johannessen, A. Olsen, R. Bellerby, C. S. Wong, B. Delille, N. R. Bates, H. J. W. de Baar, Climatological mean and decadal change in surface ocean pCO_2, and net sea–air CO_2 flux over the global oceans. *Deep Sea Res. II* **56**, 554–577 (2009).
8. S. Steph, R. Tiedemann, M. Prange, J. Groeneveld, M. Schulz, A. Timmermann, D. Nürnberg, C. Rühlemann, C. Saukel, G. H. Haug, Early Pliocene increase in thermohaline overturning: A precondition for the development of the modern equatorial Pacific cold tongue. *Paleoceanography* **25**, PA2202 (2010).
9. H. L. Ford, A. C. Ravelo, S. Hovan, A deep eastern equatorial Pacific thermocline during the early Pliocene warm period. *Earth Planet. Sci. Lett.* **355–356**, 152–161 (2012).
10. C. M. Brierley, A. V. Fedorov, Z. Liu, T. D. Herbert, K. T. Lawrence, J. P. LaRiviere, Greatly expanded tropical warm pool and weakened hadley circulation in the early Pliocene. *Science* **323**, 1714–1718 (2009).
11. A. V. Fedorov, N. J. Burls, K. T. Lawrence, L. C. Peterson, Tightly linked zonal and meridional sea surface temperature gradients over the past five million years. *Nat. Geosci.* **8**, 975–980 (2015).
12. N. J. Burls, A. V. Fedorov, What controls the mean east–west sea surface temperature gradient in the Equatorial Pacific: The role of cloud albedo. *J. Clim.* **27**, 2757–2778 (2014).
13. A. V. Fedorov, C. M. Brierley, K. T. Lawrence, Z. Liu, P. S. Dekens, A. C. Ravelo, Patterns and mechanisms of early Pliocene warmth. *Nature* **496**, 43–49 (2013).
14. M. W. Wara, A. C. Ravelo, M. L. Delaney, Permanent El Niño-like conditions during the Pliocene warm period. *Science* **309**, 758–761 (2005).
15. A. Martínez-Garcia, A. Rosell-Melé, E. L. McClymont, R. Gersonde, G. H. Haug, Subpolar link to the emergence of the modern equatorial pacific cold tongue. *Science* **328**, 1550–1553 (2010).
16. P. Molnar, M. A. Cane, El Niño's tropical climate and teleconnections as a blueprint for pre-Ice Age climates. *Paleoceanography* **17**, 1021 (2002).
17. Y. G. Zhang, M. Pagani, Z. Liu, A 12-million-year temperature history of the tropical Pacific Ocean. *Science* **344**, 84–87 (2014).
18. C. L. O'Brien, G. L. Foster, M. A. Martínez-Botí, R. Abell, J. W. B. Rae, R. D. Pancost, High sea surface temperatures in tropical warm pools during the Pliocene. *Nat. Geosci.* **7**, 606–611 (2014).
19. C. M. Brierley, A. V. Fedorov, Comparing the impacts of Miocene–Pliocene changes in inter-ocean gateways on climate: Central American Seaway, Bering Strait, and Indonesia. *Earth Planet. Sci. Lett.* **444**, 116–130 (2016).
20. X. Zhang, M. Prange, S. Steph, M. Butzin, U. Krebs, D. J. Lunt, K. H. Nisancioglu, W. Park, A. Schmittner, B. Schneider, M. Schulz, Changes in equatorial Pacific thermocline depth in response to Panamanian seaway closure: Insights from a multi-model study. *Earth Planet. Sci. Lett.* **317–318**, 76–84 (2012).
21. A. C. Ravelo, K. T. Lawrence, A. Fedorov, H. L. Ford, Comment on "A 12-million-year temperature history of the tropical Pacific Ocean". *Science* **346**, 1467 (2014).
22. K. T. Lawrence, Z. Liu, T. D. Herbert, Evolution of the eastern tropical Pacific through Plio-Pleistocene glaciation. *Science* **312**, 79–83 (2006).

23. T. D. Herbert, K. T. Lawrence, A. Tzanova, L. C. Peterson, R. Caballero-Gill, C. S. Kelly, Late Miocene global cooling and the rise of modern ecosystems. *Nat. Geosci.* **9**, 843–847 (2016).
24. P. S. Dekens, A. C. Ravelo, M. D. McCarthy, Warm upwelling regions in the Pliocene warm period. *Paleoceanogr. Paleoclimatol.* **22**, PA3211 (2007).
25. O. Seki, D. N. Schmidt, S. Schouten, E. C. Hopmans, J. S. Sinninghe Damsté, R. D. Pancost, Paleoceanographic changes in the eastern equatorial Pacific over the last 10 Myr. *Paleoceanogr. Paleoclimatol.* **27**, PA3224 (2012).
26. G. Rousselle, C. Beltran, M.-A. Sicre, I. Raffi, M. D. Rafélis, Changes in sea-surface conditions in the Equatorial Pacific during the middle Miocene–Pliocene as inferred from coccolith geochemistry. *Earth Planet. Sci. Lett.* **361**, 412–421 (2013).
27. M. S. Fantle, D. J. DePaolo, Sr isotopes and pore fluid chemistry in carbonate sediment of the Ontong Java Plateau: Calcite recrystallization rates and evidence for a rapid rise in seawater Mg over the last 10 million years. *Geochim. Cosmochim. Acta* **70**, 3883–3904 (2006).
28. M. Medina-Elizalde, D. W. Lea, M. S. Fantle, Implications of seawater Mg/Ca variability for Plio-Pleistocene tropical climate reconstruction. *Earth Planet. Sci. Lett.* **269**, 585–595 (2008).
29. J. E. Hertzberg, M. W. Schmidt, T. S. Bianchi, R. W. Smith, M. R. Shields, F. Marcantonio, Comparison of eastern tropical Pacific TEX_{86} and *Globigerinoides ruber* Mg/Ca derived sea surface temperatures: Insights from the Holocene and Last Glacial Maximum. *Earth Planet. Sci. Lett.* **434**, 320–332 (2016).
30. S. L. Ho, T. Laepple, Glacial cooling as inferred from marine temperature proxies TEX^{H}_{86} and $U^{K}37$. *Earth Planet. Sci. Lett.* **409**, 15–22 (2015).
31. P. S. Dekens, D. W. Lea, D. K. Pak, H. J. Spero, Core top calibration of Mg/Ca in tropical foraminifera: Refining paleotemperature estimation. *Geochem. Geophys. Geosyst.* **3**, 1–29 (2002).
32. P. J. Müller, G. Kirst, G. Ruhland, I. von Storch, A. Rosell-Melé, Calibration of the alkenone paleotemperature index UK'37 based on core-tops from the eastern South Atlantic and the global ocean (60°N-60°S). *Geochim. Cosmochim. Acta* **62**, 1757–1772 (1998).
33. J.-H. Kim, J. van der Meer, S. Schouten, P. Helmke, V. Willmott, F. Sangiorgi, N. Koc, E. C. Hopmans, J. S. Sinninghe Damsté, New indices and calibrations derived from the distribution of crenarchaeal isoprenoid tetraether lipids: Implications for past sea surface temperature reconstructions. *Geochim. Cosmochim. Acta* **74**, 4639–4654 (2010).
34. J. E. Tierney, M. P. Tingley, BAYSPLINE: A new calibration for the alkenone paleothermometer. *Paleoceanogr. Paleoclimatol.* **33**, 281–301 (2018).
35. J. E. Tierney, M. P. Tingley, A Bayesian, spatially-varying calibration model for the TEX_{86} proxy. *Geochim. Cosmochim. Acta* **127**, 83–106 (2014).
36. H. L. Ford, A. C. Ravelo, P. S. Dekens, J. P. LaRiviere, M. W. Wara, The evolution of the equatorial thermocline and the early Pliocene *El Padre* mean state. *Geophys. Res. Lett.* **42**, 4878–4887 (2015).
37. G. H. Haug, R. Tiedemann, R. Zahn, A. C. Ravelo, Role of Panama uplift on oceanic freshwater balance. *Geology* **29**, 207–210 (2001).
38. J. W. Farrell, I. Raffi, T. R. Janecek, D. W. Murray, M. Levitan, K. A. Dadey, K.-C. Emeis, M. Lyle, J.-A. Flores, S. Hovan, Late Neogene sedimentation patterns in the eastern equatorial Pacific Ocean. *Proc. ODP Sci. Res.* **138**, 717–756 (1995).
39. M. Lyle, J. Baldauf, Biogenic sediment regimes in the Neogene equatorial Pacific, IODP Site U1338: Burial, production, and diatom community. *Palaeogeogr. Palaeoclimatol. Palaeoecol.* **433**, 106–128 (2015).
40. L. Diester-Haas, K. Billiups, K. C. Emeis, Late Miocene carbon isotope records and marine biological productivity: Was there a (dusty) link? *Paleoceanogr. Paleoclimatol.* **21**, PA4216 (2006).
41. Y. G. Zhang, M. Pagani, J. Henderiks, H. Ren, A long history of equatorial deep-water upwelling in the Pacific Ocean. *Earth Planet. Sci. Lett.* **467**, 1–9 (2017).
42. K. A. Jacob, C. T. Bolton, P. A. Wilson, A. Bahr, J. Pross, J. Fiebig, K. Kähler, O. Friedrich, Glacial–interglacial changes in equatorial Pacific surface-water structure during the Plio–Pleistocene intensification of Northern Hemisphere Glaciation. *Earth Planet. Sci. Lett.* **463**, 69–80 (2017).
43. D.-Z. Sun, The heat sources and sinks of the 1986–87 El Niño. *J. Clim.* **13**, 3533–3550 (2000).
44. R. A. Locarnini, A. V. Mishonov, J. I. Antonov, T. P. Boyer, H. E. Garcia, O. K. Baranova, M. M. Zweng, C. R. Paver, J. R. Reagan, D. R. Johnson, M. Hamilton, D. Seidov, in *NOAA Atlas NESDIS 73* (NOAA, 2013).
45. J. A. Carton, B. S. Giese, A reanalysis of ocean climate using simple ocean data assimilation (SODA). *Mon. Weather Rev.* **136**, 2999–3017 (2008).
46. R. Schlitzer, Data analysis and visualization with ocean data view. *CMOS Bull. SCMO* **43**, 9–13 (2015).
47. J. Tian, X. Ma, J. Zhou, M. Lyle, J. Shackford, R. Wilkens, Paleoceanography of the east equatorial Pacific over the past 16 Myr and Pacific–Atlantic comparison: High resolution benthic foraminiferal $\delta^{18}O$ and $\delta^{13}C$ records at IODP Site U1337. *Earth Planet. Sci. Lett.* **499**, 185–196 (2018).
48. J. T. Pennington, K. L. Mahoney, V. S. Kuwahara, D. D. Kolber, R. Calienes, F. P. Chavez, Primary production in the eastern tropical Pacific: A review. *Prog. Oceanogr.* **69**, 285–317 (2006).
49. M. Seton, R. D. Müller, S. Zahirovic, C. Gaina, T. Torsvik, G. Shephard, A. Talsma, M. Gurnis, M. Turner, S. Maus, M. Chandler, Global continental and ocean basin reconstructions since 200 Ma. *Earth Sci. Rev.* **113**, 212–270 (2012).
50. K. J. Matthews, K. T. Maloney, S. Zahirovic, S. E. Williams, M. Seton, R. D. Müller, Global plate boundary evolution and kinematics since the late Paleozoic. *Glob. Planet. Chang.* **146**, 226–250 (2016).
51. M. Mudelsee, Ramp function regression: A tool for quantifying climate transitions. *Comput. Geosci.* **26**, 293–307 (2000).
52. J. P. LaRiviere, A. C. Ravelo, A. Crimmins, P. S. Dekens, H. L. Ford, M. Lyle, M. W. Wara, Late Miocene decoupling of oceanic warmth and atmospheric carbon dioxide forcing. *Nature* **486**, 97–100 (2012).

Acknowledgments: We thank IODP for providing samples for this study and IODP China office for additional support. We also thank Y. Wang for help in retrieving SODA data. **Funding:** This research was financially supported by the National Natural Science Foundation of China (grant nos. 41525020, 41776051, and 91428310), the Shanghai Human Development Fund (201336), and the Program of Shanghai Subject Chief Scientist (A type) (16XD1403000) to J.T. and by the Hong Kong Research Grants Council (17303614) to Z.L. A.V.F. was supported by the Guggenheim Fellowship. T.D.H. was supported by NSF-OCE-0623487. **Author contributions:** J.T. and Z.L. designed the research; J.L. performed alkenone analysis; and T.D.H., M.L., and A.V.F. assessed aspects of surface temperature, biological production, and theoretical concerns, respectively. All authors contributed to interpreting the data and writing the paper. **Competing interests:** The authors declare that they have no competing interests. **Data and materials availability:** All data needed to evaluate the conclusions in the paper are present in the supplementary tables. Additional data related to this paper may be requested from the authors.

Submitted 27 June 2018
Accepted 12 February 2019
Published 3 April 2019
10.1126/sciadv.aau6060

Citation: J. Liu, J. Tian, Z. Liu, T. D. Herbert, A. V. Fedorov, M. Lyle, Eastern equatorial Pacific cold tongue evolution since the late Miocene linked to extratropical climate. *Sci. Adv.* **5**, eaau6060 (2019).